Antenna Miniaturization with MEMS Tunable Capacitors

Techniques and Trade-offs

Barrio, Samantha Caporal Del; Morris, Art; Pedersen, Gert Frølund

Published in:
International Journal of Antennas and Propagation

DOI (link to publication from Publisher):
10.1155/2014/709580

Publication date:
2014

Document Version
Early version, also known as pre-print

Hindawi Publishing Corporation
International Journal of Antennas and Propagation
Volume 2014, Article ID 709580, 8 pages
http://dx.doi.org/10.1155/2014/709580

Research Article

Antenna Miniaturization with MEMS Tunable Capacitors: Techniques and Trade-Offs

Samantha Caporal Del Barrio,[1,2] Art Morris,[2] and Gert F. Pedersen[1]

[1] *Section of Antennas, Propagation and Radio Networking (APNet), Department of Electronic Systems, Faculty of Engineering and Science, Aalborg University, Denmark*
[2] *WiSpry Inc., 20 Fairbanks, Suite 198, Irvine, CA 92618, USA*

Correspondence should be addressed to Samantha Caporal Del Barrio; scdb@es.aau.dk

Received 2 May 2014; Revised 1 July 2014; Accepted 4 July 2014; Published 20 August 2014

Academic Editor: Yingsong Li

In today's mobile device market, there is a strong need for efficient antenna miniaturization. Tunable antennas are a very promising way to reduce antenna volume while enlarging its operating bandwidth. MEMS tunable capacitors are state-of-the-art in terms of insertion loss. Their characteristics are used in this investigation. This paper uses field simulations to highlight the trade-offs between the design of the tuner and the design of the antenna, especially the impact of the location of the tuner and the degree of miniaturization. Codesigning the tuner and the antenna is essential to optimize radiated performance.

1. Introduction

With their increasing functionality, mobile phones are embedding better screens, better cameras, larger batteries, and more antennas, among others. In order to keep the portability of such device, a very high degree of integration is required. Chipset miniaturization has seen a large success over the last years [1]; however, antenna volume is ruled by fundamental laws [2] that relate size, efficiency, and bandwidth. To support the latest mobile communication standards, long-term evolution (LTE), and LTE-advanced (LTE-A), the antennas need to operate in frequency bands ranging from 698 MHz to 2.690 GHz. In order to maintain good performance throughout such a large bandwidth with a conventional design, the antenna volume must be increased.

Nowadays, the most common types of antenna designs for mobile phones are classified into two categories: self-resonating elements and nonresonating elements (also known as capacitive coupling elements). Self-resonating multiband antennas can cover several bands simultaneously. Literature reports a coverage up to 9 simultaneous bands. These antennas are space consuming as the antenna volume increases nearly linearly with the number of bands supported. For example, [3] occupies a volume of 4.6 cc to cover all GSM bands, the antenna presented in [4] covers the GSM, DCS, PCS, and UMTS bands in a volume of 1.9 cc, and [5] needs about 7 cc to also include GPS, Bluetooth, WLAN, AMPS, and DVB-H bands. Nonresonating antennas exhibit a lower profile and exploit the ground plane modes to obtain a large bandwidth. Hence, covering the lowest LTE band is possible. However, this type of antennas typically uses several matching components at the feed, which affects the total efficiency. For example, [6] covers down to 700 MHz in 2.5 cc, but with a total efficiency dropping to 55%. Additionally, nonresonating antennas fully utilize the ground plane, which complicates decoupling, required for the multiple-input multiple-output (MIMO) technique in LTE and LTE-A.

Modern phones have antennas that exhibit a very low profile, at the cost of their performance. The investigation in [7] shows total radiated power (TRP) and total isotropic sensitivity (TIS) values in the presence of hand and head phantoms, for popular smart-phones in 2012. For example, TRP ranges from 16.6 dBm to 20.1 dBm in the GSM-900 band. Before 2000, handsets with a patch antenna performed with TRP values of about 26 dBm [8], in the presence of a user for GSM-900. Today's phones exhibit poor antenna efficiency, it

can be as low as −7.7 dB [9] in free space. This phenomenon is due to the ever increasing number of bands to cover the constrained space available for the antenna. It has led to antenna designs exhibiting a wide but mismatched antenna impedance [9]. Efficient miniaturization has not happened yet in commercial devices.

To address the bandwidth-size challenge of modern antennas, tunable antennas are investigated. They use a tunable component in order to reconfigure their resonance frequency. These antennas exhibit an instantaneous narrow bandwidth, that can be reconfigured to a wide range of frequencies, thus resulting in an effectively wide bandwidth. As the antenna is designed for a narrow bandwidth, it can have a very low profile. In the architecture proposed in [10], the antenna only needs to cover a channel (maximum 20 MHz in LTE and LTE-A). Exploiting the narrow-band property of tunable antennas, very compact designs can be made. In [10], the radiators only occupy 1.0 cc and cover operating bands between 600 MHz and 2.1 GHz. Tunable antennas have a tremendous potential for miniaturization.

The performance of tunable antennas is tested over-the-air [11] and relies on an efficient codesign of the radiator and the tuner. The objective of this paper is to investigate the trade-offs and the requirements between the antenna designers and the tuner designers. Codesigning the antenna and the tuner is essential to manufacture small and efficient tunable antennas. Section 2 compares the different tuning technologies. Section 3 describes the impacts of the location of the tuner on the antenna design. Section 4 investigates the requirements on the tuner for different levels of miniaturization. Finally, Section 5 discloses the conclusions.

2. Tuning Elements

Because reconfiguring the resonance frequency of an antenna allows to extend its operating bandwidth without modifying its physical size, tunable antennas are very promising to address the antenna miniaturization challenge. There are several components that can be used to tune the resonance frequency of an antenna. To name the most common ones, there are switched capacitors, tunable substrates, and micro-electromechanical Systems (MEMS).

The switching approach combines a single-pole-multiple-throw (SPnT) switch and a bank of capacitors to choose from. It uses most commonly field effect transistors (FET) which leads to an intrinsically low breakdown voltage and power handling, limiting its application to mobile communication standards [12]. PIN diodes can handle more power; however, they exhibit a higher insertion loss, a smaller tuning range, and a higher power consumption [13].

Tunable substrates (also known as paraelectric solutions) provide variable capacitance without the need for a FET switch, thus increasing the quality factor (Q) of the component. It uses barium strontium titanate (BST) which causes the design to have issues with linearity.

In the mechanism of MEMS tunable capacitors, an electrostatic force actuates a beam. When the beam is down, only dielectric separates it from the metal trace below it and the capacitor is *on*. When the beam is up, an additional air gap separates the beam from the metal trace and the capacitor is *off* [12]. With this architecture, the RF path is a metal trace. Therefore, MEMS capacitors offer significantly higher Q and linearity than the previous solutions. Additionally, the structure of the component allows for the handling of higher voltages. Tunability can also be realized using varactors, as in [14–17]. However, the limit on maximum achievable capacitance and the high bias voltage requirements reduce the flexibility of such tuning technique.

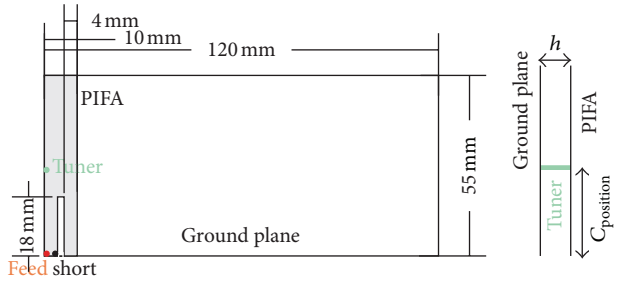

Figure 1: Antenna design used to investigate the impact of $C_{position}$.

MEMS tunable solutions are state-of-the-art in terms of insertion loss and power consumption. The following investigations are made considering that the tuner is a MEMS tunable capacitor. More specifically, a commercially available tuner is used [18] that exhibits a tuning range from 1 pF to 4.875 pF with steps of 125 fF.

3. Tuner Location Trade-Offs

In order to reconfigure the resonance frequency of an antenna, one can choose to place a tuner at different locations. These locations depend on the antenna type and the tuning objectives. In the case of antennas based on wideband coupling elements, the tuner is typically placed at the feed to match the antenna to different operating frequencies simultaneously [6, 19–21] or instantaneously [22–25]. Frequency reconfigurability can also be achieved by loading the antenna structure itself [26–28] or by placing the tuner between the antenna element and the ground plane [29–35]. The latter is the most common use of tunable MEMS capacitors; therefore, this placement will be used for the following investigation. The following is illustrated with a low-band design.

3.1. Simulation Results. The antenna design described in Figure 1 is chosen for this investigation. Simulations are conducted with the transient solver, based on finite-element method (FEM), of the CST software [36]. It is a typical planar-inverted-F antenna (PIFA) for mobile phone application and addresses the low-bands of LTE, 698 MHz to 960 MHz. The position of the tuner ($C_{position}$) is given in mm away from the feed, at the edge of the antenna and the ground plane. The instantaneous bandwidth of the antenna is determined by the height of the PIFA above the ground plane (h). When h = 2 mm, the bandwidth of the antenna, at −6 dB return loss, equals 34 MHz, centered in 960 MHz. The initial resonance

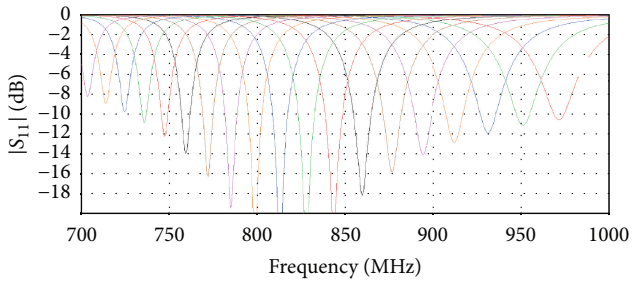

Figure 2: Antenna tuning, with tuner placed in $C_{\text{position}} = 20$ mm.

frequency of the proposed design is 960 MHz, as it is the high bound of the low bands of 4 G. Tuning enables it to cover the 261 MHz required for LTE, as shown with the simulations of Figure 2. This design uses a tunable capacitor placed at the position $C_{\text{position}} = 20$ mm, providing varying capacitance from 1 pF to 4.875 pF.

The location of the tuner on the antenna structure has an impact on the specifications required for the MEMS tunable capacitor, that is, insertion loss (L_{ins}), voltage across the tuner (V_{tuner}), tuning step (C_{step}), and maximum capacitance (C_{max}). The insertion loss of the tuner depends on its maximum equivalent series resistance (ESR_{max}) and the current that flows to it.

In this investigation, it has been set that the efficiency should be better or equal to 50% throughout the operable bandwidth. This means that $L_{\text{ins}} = 3$ dB at 700 MHz, low bound of 4 G bands. Indeed, the antenna radiation efficiency degrades as it is tuned further away from its original resonance frequency. That is because higher fields concentrate around the antenna structure, inducing larger currents to the capacitor. Therefore, larger currents to the ESR of the capacitor cause higher loss. Hence, the lowest efficiency is observed at the lowest operating frequency of the tunable antenna. With $L_{\text{ins}} = 3$ dB at 700 MHz, L_{ins} will be equal to 2 dB at 800 MHz and 1 dB at 900 MHz.

In order to demonstrate the trade-offs linked to the position of the tuner on the antenna, different locations of the tuner are simulated and compared. The position of the tuner varies in arbitrary steps from 5 mm away from the feed (high current location) to 55 mm away from the feed (high voltage location). The antenna is continuously tuned from 960 MHz to 700 MHz. The requirements on the tuner, depending on its location, are summarized in Table 1, for 700 MHz, where the requirements are the toughest, since the fields are the highest. It is observed that the requirements on V_{tuner} and C_{step} are toughened as the tuner is placed further away from the feed. Similarly, the requirements on the C_{max} and ESR_{max} are toughened as the tuner is placed closer to the feed. Indeed, as C_{position} decreases, the current flowing to the capacitor increases and the ESR of the tuner dissipates more power. Thus, it needs to be smaller to keep the efficiency at 50%. One can notice that the impact of the tuner location on the tuner design is significant, as its requirements on V_{tuner} and ESR_{max} are nearly quadrupled, and its requirements on C_{step} are nearly ten times toughened. Moreover, if the V_{tuner} allows it, the most efficient location for a tuner is the furthest from the feed, as the power dissipation due to the ESR will be minimized. Therefore, this location is used for the investigation of Section 4. The achievable bandwidth only varies by 1 MHz, depending on the different locations of the tuner.

Table 1: Trade-offs due to location of the tuner.

C_{position} [mm]	5	10	15	30	55
f_r [MHz]	700	700	700	700	700
L_{ins} [dB]	3	3	3	3	3
ESR_{max} [Ω]	0.41	0.58	0.80	1.13	1.48
V_{tuner} [V]	30	41	53	80	97
C_{step} [pF]	0.9	0.6	0.4	0.2	0.1
C_{max} [pF]	11.4	7.2	4.8	2.7	1.9

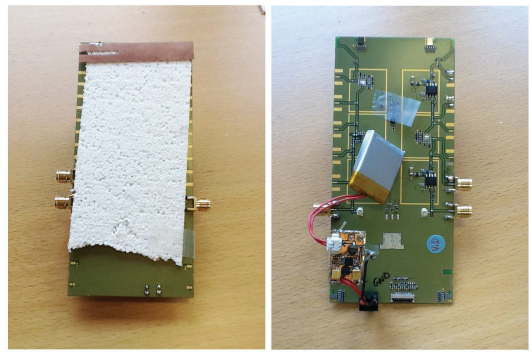

Figure 3: Low-band demonstrator, tuner placed in $C_{\text{position}} = 10$ mm. The tuner has a minimum capacitance of 1 pF and a maximum capacitance of 4.875 pF.

3.2. Measurement Results. A demonstrator of the presented antenna is built and shown in Figure 3. The tuner was placed at $C_{\text{position}} = 10$ mm due to schematic limitations on the demonstrator board. This position only allows for the tuning of the antenna to 800 MHz, with a tuner exhibiting 4.875 pF tuning range. Continuous tuning is shown in Figure 4. The demonstrator was measured in Satimo StarLab and exhibited a total efficiency (η_T) of −2.0 dB at 900 MHz and −3.2 dB at 800 MHz. The η_T includes mismatch loss and 0.8 dB of trace loss. Improvements in the ESR will directly improve the measured η_T.

4. Antenna Miniaturization Trade-Offs

4.1. Theory. The antenna quality factor (Q_{ant}) is a measure that can be translated into antenna volume, stored energy, or bandwidth. These relations are detailed in [37]. In order to understand the trade-offs of miniaturization, one needs to understand the consequences of decreasing antenna volume on the Q_{ant}.

Q_{ant} relates to volume as follows [38]:

$$Q_{\text{ant}}(\omega) = \left(\frac{1}{(ka)^3} + \frac{1}{ka}\right), \quad (1)$$

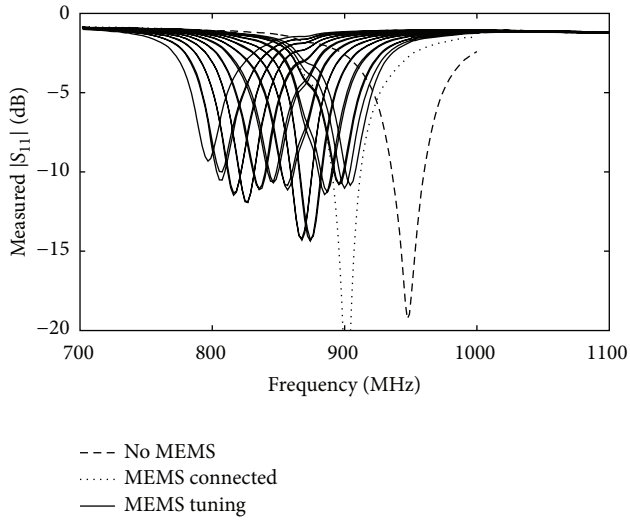

Figure 4: Measured frequency response of the demonstrator shown in Figure 3, with $C_{max} = 4.875$ pF and $C_{step} = 125$ fF.

where a is the radius of an imaginary sphere circumscribing the maximum dimension of the antenna and k is the wave number. As the volume occupied by the antenna decreases the Q_{ant} increases, at a given angular frequency (ω). The Q_{ant} is also related to the instantaneous bandwidth of the antenna, for single resonance antennas. The relationship between Q_{ant} and fractional bandwidth (FBW) is [37]

$$Q_{ant}(\omega) = \frac{2\sqrt{\beta}}{\mathrm{FBW}_{VSWR}(\omega)}, \quad \sqrt{\beta} = \frac{s-1}{2\sqrt{s}}, \tag{2}$$

where FBW_{VSWR} is the FBW matched to a voltage standing wave ratio (VSWR) and s is the specific value of the VSWR. The antenna bandwidth is inversely proportional to Q_{ant}. Thus, the volume is proportional to the antenna bandwidth. That is to say, when the antenna volume decreases, the bandwidth does as well. Finally, the Q_{ant} is also a measure of the stored energy (W) in the antenna structure versus the accepted power (P_A) [37]

$$Q_{ant}(\omega) = \frac{\omega |W(\omega)|}{P_A(\omega)}. \tag{3}$$

Therefore, the larger the Q_{ant}, the larger the stored energy. Thus, larger fields are confined in the antenna structure. Consequently, larger currents and voltages flow to the tuner, impacting insertion loss and voltage handling. To sum up, as the antenna becomes smaller, its bandwidth decreases and the tuning capacitor needs to have better characteristics in order to cope with the increased fields.

4.2. Example. The above is illustrated using a high-band design to emphasize how small an antenna can get. In the following, a design addressing band 41 [2.496 GHz–2.690 GHz] will be presented and used for the miniaturization investigation. The antenna is placed on a 120 mm × 55 mm ground plane and its geometry is described in Figure 5. Simulations are conducted using the transient solver of CST [36]. Three ports are placed on the antenna, where port 1 represents the feed, port 2 presents the tuner, and port 3 presesnts the short. The tuner is placed the furthest form the feed, given the results of Section 3. The design is modified in order to have four different models with four different initial bandwidths. The width of the top plate (W) and its height (H) are the main parameters controlling the bandwidth of the antenna, that is, Q_{ant}. The length parameter (L) varies accordingly, in order to adjust the initial resonance to 2.690 GHz. Five antenna designs are simulated (D0–D4), with initial bandwidths varying from 168 MHz to 32 MHz. The geometry required for each of these cases is described in Table 2. The characteristics of the five designs are summarized in Table 3, especially the volume, the bandwidth at the high bound of band 41 ($\mathrm{BW}_{2.7GHz}$), and the bandwidth at 2.400 GHz ($\mathrm{BW}_{2.4GHz}$). Implementing tuning allows to have tremendously small antenna designs; for example, D4 is ten times smaller than D1 and still cover the required band with tuning.

Table 2: Antenna geometry.

Parameters [mm]	D0	D1	D2	D3	D4
L	10	3.8	3.8	4.8	7.5
H	2.0	5.0	4.0	3.0	1.0
W	5.0	5.0	5.0	2.0	1.0
w	5.0	2.0	2.0	2.0	1.0
h	1.0	1.0	1.0	1.0	1.0
d	4.0	1.5	1.0	1.0	0.6

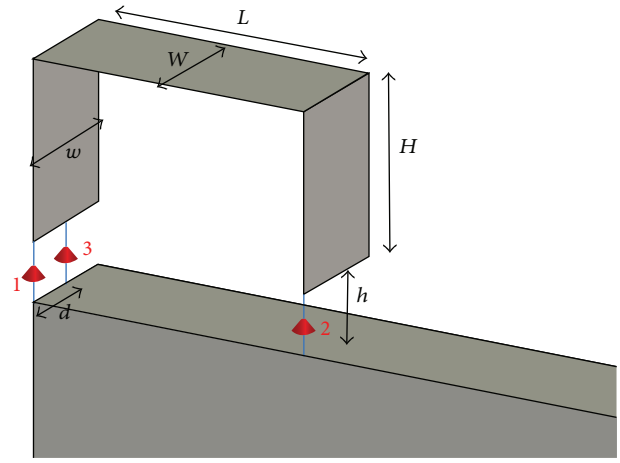

Figure 5: High-band antenna design.

All four designs are tuned to 2.400 GHz. As the antenna becomes narrow-band, that is, smaller, it will store higher fields and impact the L_{ins} and V_{tuner}. In order to maintain 50% total efficiency at 2.400 GHz, the ESR_{max} needs to decrease as the bandwidth decreases. D4 occupies 1/10 of the volume of D1 and needs an ESR_{max} four times smaller. Simultaneously, the V_{tuner} needs to increase as the antenna becomes smaller. D4 requires a V_{tuner} three times larger. The results are summarized in Table 4. Both the antenna volume and the ESR

Table 3: Design characteristics.

	D0	D1	D2	D3	D4
Volume [cc]	0.15	0.11	0.09	0.04	0.01
$BW_{2.7GHz}$ [MHz]	168	118	78	62	32
$BW_{2.4GHz}$ [MHz]	119	84	61	46	23

Table 4: Tuner requirements.

	D0	D1	D2	D3	D4
f_r [GHz]	2.400	2.400	2.400	2.400	2.400
L_{ins} [dB]	3	3	3	3	3
ESR_{max} [Ω]	4.5	3.2	2.5	1.5	0.8
V_{tuner} [V]	10	10	10	17	31

Table 5: Q comparisons at 2.400 GHz.

	D0	D1	D2	D3	D4
Q_{ant}	16	23	25	47	97
Q_{MEMS}	35	35	45	75	142

of the tuner can be expressed in terms of Q values. Q_{ant} is calculated using (2). It is the unloaded Q_{ant}, meaning that it is calculated based on a lossless simulation. Table 5 compares the Q values between the antenna design and the MEMS capacitor design leading to 3 dB L_{ins}. The Q_{MEMS} is calculated as detailed in (4), where C is the capacitance. It is observed that the ratio between Q_{MEMS} and Q_{ant} leading to 50% total efficiency is nearly constant and equals 1.5

$$Q_{MEMS}(\omega) = \frac{1}{\omega \times C \times ESR}. \quad (4)$$

4.3. Measurements

(1) High-Band Tuning. A demonstrator is built for the design D0, as it is shown in Figure 6. The dimensions of the board are 120 mm × 55 mm. In practice, the antenna is soldered directly on the feeding pad of the board; therefore, h = 0 mm. The tuner is a MEMS tunable capacitor [18] and it is connected to the antenna from the other side of the board. In order to deal with the small minimum capacitance (C_{min}) required for the proposed designed, a series capacitor is placed between the antenna and the tuner according to the schematics depicted in Figure 7. The series capacitor has a value of 0.6 pF, which decreases the C_{min} from 1 pF (original value for the commercial tuner) to 0.375 pF. Moreover, the addition of the series capacitor decreases V_{tuner}.

Continuous tuning from 2.7 GHz (high bound of 4 G) to 2.4 GHz (WiFi) is shown in Figure 8. On can see that, as the antenna is tuned further away from its natural resonance frequency, the tuning steps are reduced. This is due to the insertion of the series capacitor. The η_T of the demonstrator was measured with 3D-pattern integration tehnique using Satimo StarLab. The results are shown for three tuning stages in Figure 9. Due to the low Q_{ant} (wide bandwidth) and the position of the tuner (furthest from the feed), fields strength

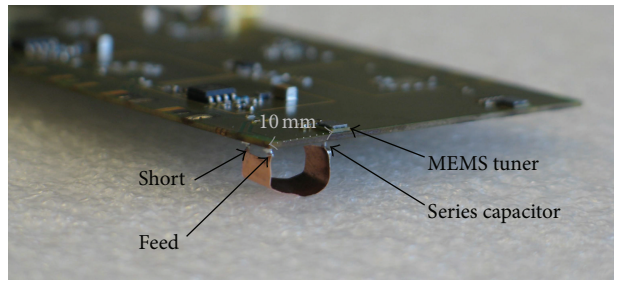

Figure 6: High-band demonstrator.

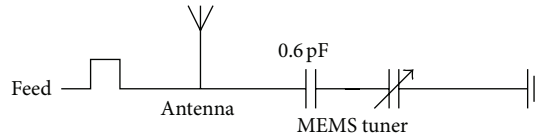

Figure 7: Schematic of the high-band demonstrator.

is kept low and the demonstrator is efficient. Moreover, the efficiency remains quasiconstant throughout tuning: −2.0 dB to −2.5 dB. It includes mismatch loss and trace loss on the board (0.8 dB).

(2) Miniaturization. Using the design techniques of the above-presented antennas, a new design is built to address the low bands of 4 G. This design is identical to D0, except for H that is equal to 10 mm instead of 5 mm. The electrical dimensions of the antenna are electrically small. At 700 MHz, the maximum antenna dimension (10 mm) represents 1/42th of the wavelength. This experiment tests the limitations of miniaturization.

Given the tuner properties (tuning range from 1 pF to 4.875 pF [18]), an additional fixed capacitor is placed in series with the tuner, in order to have enough capacitance to reach 700 MHz. The schematic is shown in Figure 10.

The demonstrator is shown in Figures 11 and 12. The antenna volume is 0.5 cc for operation in the low LTE bands. The frequency reconfigurability of the antenna is plotted in Figure 13 and shows continuous tuning from 940 MHz to 700 MHz. With the operating frequencies being very far from the natural resonance frequency of the antenna design, the unloaded Q_{ant} is very large. It is simulated to be larger than 300, which means that the antenna is very sensitive to the insertion loss of the tuner. The demonstrator is measured in the Satimo StarLab and η_T is computed with 3D-pattern integration technique. The results are shown in Figure 14 for three different tuning stages. The η_T includes the mismatch loss (less than 0.5 dB) and the loss of the traces in the board (0.8 dB). Efficiency degradation is observed as the antenna is tuned towards lower frequencies. For the lowest operating frequencies, the η_T reaches −11 dB. The limitation of miniaturization with tuners is the achievable efficiency of the system. The cause of loss is twofold: the metal loss due to nonperfect conductor (copper) and the ESR loss due to increasing Q_{ant} and field strength around the tuner, thus currents in the ESR. The net ESR of the tuner and interconnects used on the board

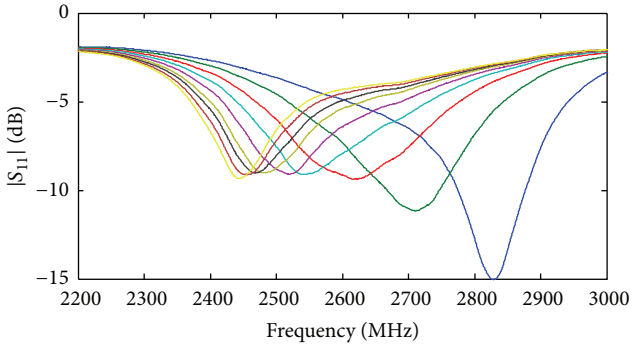

Figure 8: Measured tuning range of the demonstrator in Figure 6.

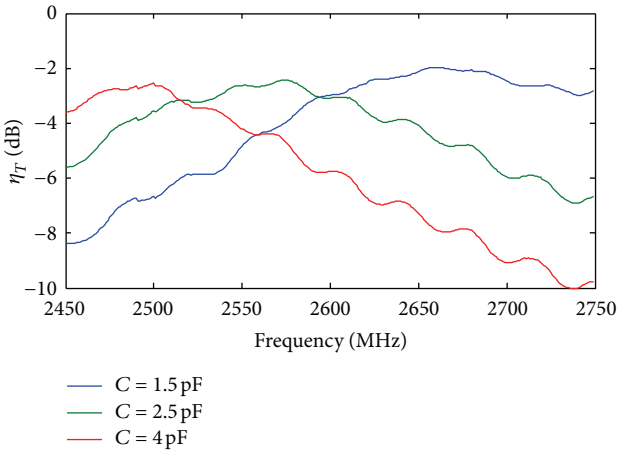

Figure 9: Measured total efficiency of the demonstrator in Figure 6.

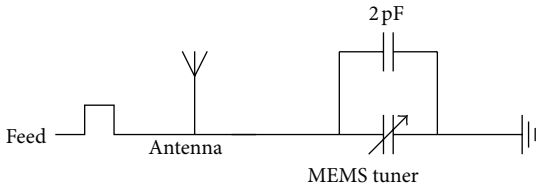

Figure 10: Schematic of the miniaturization demonstrator.

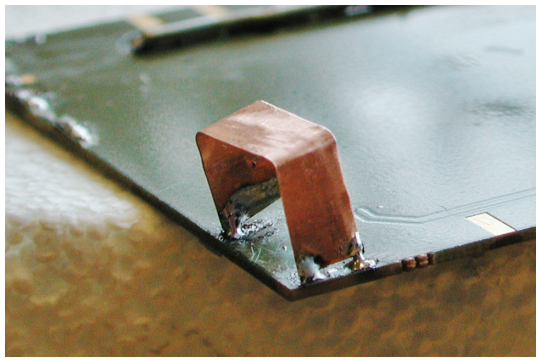

Figure 11: Antenna miniaturization demonstrator, top view.

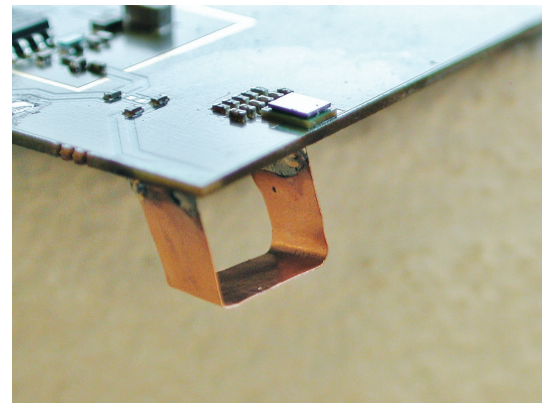

Figure 12: Antenna miniaturization demonstrator, bottom view.

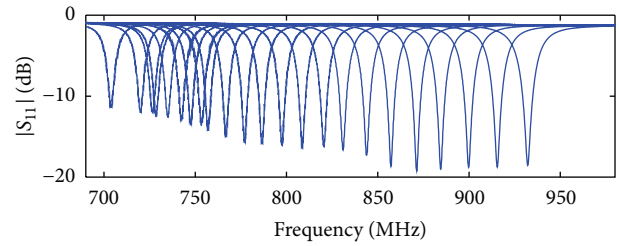

Figure 13: Measured tuning range of the demonstrator in Figure 11.

is equal to 2Ω and causes most of the loss for this very high Q antenna. Thus, the efficiency will significantly improve by using a newer generation of tuners that exhibits a lower ESR along with improvements in the interconnects. In order to get a loss of 3 dB at 700 MHz for the proposed design, the effective ESR should be reduced to 0.2Ω.

5. Conclusion

This work has detailed the interdependency of the antenna design and the tuner design. The presented investigations have highlighted the importance of codesigning the tuner and the antenna. Examples have been given for a low-band antenna design as well as for a high-band antenna design. The design trade-offs come from two sources. On one hand, the required characteristics of the tunable capacitor relate to its location on the antenna. On the other hand, they relate to the antenna initial bandwidth, in other words the Q_{ant}. Depending on its application, the tunable antenna will require a certain volume and, together with the location of the tuner, they will determine a set of tuner parameters (ESR, voltage handling and maximum capacitance) to realize an optimized design. The required characteristics of the tuner are strongly dependent on its location; for example, the required capacitance steps can be up to 10 times smaller, if placed far from the feed.

Using tunable components, the antenna volume can be dramatically decreased and the efficiency can remain above 50% as long as the ratio between Q_{MEMS} and the unloaded Q_{ant} is about 1.5. Demonstrators have been built supporting

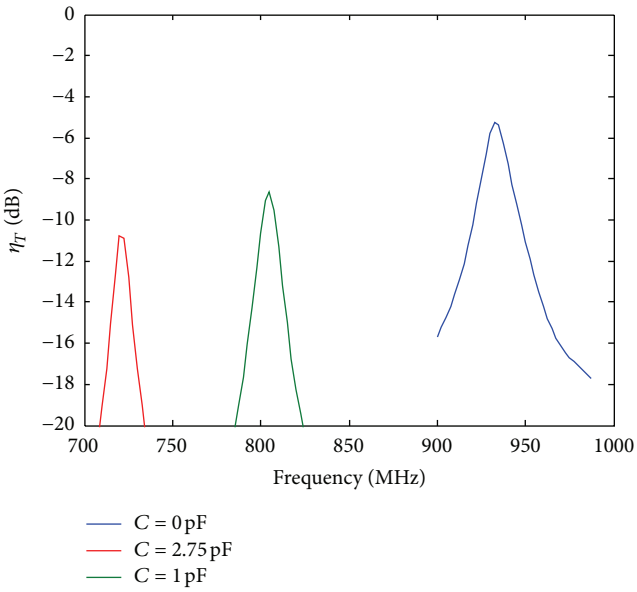

Figure 14: Measured total efficiency of the demonstrator in Figure 11.

the investigation on codesigning trade-offs. Efficiency of tunable antennas can be optimized. The limits of miniaturization lie in the achievable antenna efficiency, which determines the feasibility of the system. Improvements in tuner insertion loss will directly improve the total efficiency of tunable antennas and highlight their tremendous potential for miniaturization.

Conflict of Interests

The authors declare that there is no conflict of interests regarding the publication of this paper.

References

[1] D. Vye, "The economics of handset RF front-end integration," *Microwave Journal*, vol. 53, pp. 22–67, 2010.

[2] R. F. Harrington, "Effect of antenna size on gain, bandwidth, and efficiency," *Journal of Research of the National Bureau of Standards D: Radio Propagation*, vol. 64, no. 1, pp. 1–12, 1960.

[3] Y. Guo, M. Y. W. Chia, and Z. N. Chen, "Miniature built-in quad-band antennas for mobile handsets," *IEEE Antennas and Wireless Propagation Letters*, vol. 2, no. 10, pp. 30–32, 2003.

[4] H. Rhyu, J. Byun, F. J. Harackiewicz et al., "Multi-band hybrid antenna for ultra-thin mobile phone applications," *Electronics Letters*, vol. 45, no. 15, pp. 773–774, 2009.

[5] K. R. Boyle and P. J. Massey, "Nine-band antenna system for mobile phones," *Electronics Letters*, vol. 42, no. 5, pp. 265–266, 2006.

[6] J. Ilvonen, P. Vainikainen, R. Valkonen, and C. Icheln, "Inherently non-resonant multi-band mobile terminal antenna," *Electronics Letters*, vol. 49, no. 1, pp. 11–13, 2013.

[7] A. Tatomirescu and G. F. Pedersen, "Body-loss for popular thin smart phones," in *Proceedings of the 7th European Conference on Antennas and Propagation (EuCAP '13)*, pp. 3754–3757, April 2013.

[8] G. F. Pedersen and J. Ø. Nielsen, "Radiation pattern measurements of mobile phones next to different head phantoms," in *Proceedings of the 13th IEEE International Symposium on Personal, Indoor and Mobile Radio Communications (PIMRC '02)*, vol. 4, pp. 1888–1892, September 2002.

[9] S. Caporal Del Barrio and G. F. Pedersen, "Correlation evaluation on small LTE handsets," in *Proceedings of the 76th IEEE Vehicular Technology Conference (VTC '12)*, pp. 1–4, September 2012.

[10] S. C. del Barrio, A. Tatomirescu, G. F. Pedersen, and A. Morris, "Novel architecture for LTE world-phones," *IEEE Antennas and Wireless ropagation Letters*, vol. 12, no. 1, pp. 1676–1679, 2013.

[11] W. Fan, X. C. B. de Lisbona, F. Sun, J. O. Nielsen, M. B. Knudsen, and G. F. Pedersen, "Emulating spatial characteristics of MIMO channels for OTA testing," *IEEE Transactions on Antennas and Propagation*, vol. 61, no. 8, pp. 4306–4314, 2013.

[12] V. Steel and A. Morris, "Tunable RF Technology Overview," 2012.

[13] R. Cory and D. Fryklund, "Solid State RF/Microwave Switch Technology: Part 2," 2009.

[14] S. K. Oh, H. S. Yoon, and S. O. Park, "A PIFA-type varactor-tunable slim antenna with a PIL patch feed for multiband applications," *IEEE Antennas and Wireless Propagation Letters*, vol. 6, no. 11, pp. 103–105, 2007.

[15] N. Behdad and K. Sarabandi, "A varactor-tuned dual-band slot antenna," *IEEE Transactions on Antennas and Propagation*, vol. 54, no. 2, pp. 401–408, 2006.

[16] N. Behdad and K. Sarabandi, "Dual-band reconfigurable antenna with a very wide tunability range," *IEEE Transactions on Antennas and Propagation*, vol. 54, no. 2, pp. 409–416, 2006.

[17] L. M. Feldner, C. T. Rodenbeck, C. G. Christodoulou, and N. Kinzie, "Electrically small frequency-agile PIFA-as-a-package for portable wireless devices," *IEEE Transactions on Antennas and Propagation*, vol. 55, no. 11, pp. 3310–3319, 2007.

[18] WiSpry Tunable Digital Capacitor Arrays (TDCA), http://www.wispry.com/products-capacitors.php.

[19] A. Cihangir, F. Sonnerat, F. Ferrero et al., "Neutralisation technique applied to two coupling element antennas to cover low LTE and GSM communication standards," *Electronics Letters*, vol. 49, no. 13, pp. 781–782, 2013.

[20] A. Cihangir, F. Ferrero, C. Luxey, G. Jacquemod, and P. Brachat, "A bandwidth-enhanced antenna in LDS technology for LTE700 and GSM850/900 standards," in *Proceedings of the 7th European Conference on Antennas and Propagation (EuCAP '13)*, pp. 2786–2789, April 2013.

[21] A. Lehtovuori, R. Valkonen, and M. Valtonen, "Accessible approach to wideband matching," in *Proceedings of the 19th IEEE International Conference on Electronics, Circuits, and Systems, (ICECS '12)*, pp. 244–247, December 2012.

[22] D. Manteuffel and M. Arnold, "Considerations for reconfigurable multi-standard antennas for mobile terminals," in *Proceedings of the International Workshop on Antenna Technology: Small Antennas and Novel Metamaterials (iWAT '08)*, pp. 231–234, Chiba, Japan, March 2008.

[23] L. Huang and P. Russer, "Electrically tunable antenna design procedure for mobile applications," *IEEE Transactions on Microwave Theory and Techniques*, vol. 56, no. 12, pp. 2789–2797, 2008.

[24] R. Valkonen, C. Luxey, J. Holopainen, C. Icheln, and P. Vainikainen, "Frequency-reconfigurable mobile terminal antenna with MEMS switches," in *Proceedings of the 4th*

European Conference on Antennas and Propagation (EuCAP '10), pp. 1–5, April 2010.

[25] R. Valkonen, J. Holopainen, C. Icheln, and P. Vainikainen, "Broadband tuning of mobile terminal antennas," in *Proceeding of the IET Seminar Digests*, p. 182, IET, 2007.

[26] E. Erdil, K. Topalli, M. Unlu, O. A. Civi, and T. Akin, "Frequency tunable microstrip patch antenna using RF MEMS technology," *IEEE Transactions on Antennas and Propagation*, vol. 55, no. 4, pp. 1193–1196, 2007.

[27] V.-A. Nguyen, R.-A. Bhatti, and S. Park, "A simple PIFA-based tunable internal antenna for personal communication handsets," *IEEE Antennas and Wireless Propagation Letters*, vol. 7, pp. 130–133, 2008.

[28] Y. K. Park and Y. Sung, "A reconfigurable antenna for quad-band mobile handset applications," *IEEE Transactions on Antennas and Propagation*, vol. 60, no. 6, pp. 3003–3006, 2012.

[29] K. R. Boyle and P. G. Steeneken, "A five-band reconfigurable PIFA for mobile phones," *IEEE Transactions on Antennas and Propagation*, vol. 55, no. 11, pp. 3300–3309, 2007.

[30] J. R. de Luis, A. Morris, Q. Gu, and F. de Flaviis, "Tunable duplexing antenna system for wireless transceivers," *IEEE Transactions on Antennas and Propagation*, vol. 60, no. 11, pp. 5484–5487, 2012.

[31] Q. Gu and J. R. de Luis, "RF MEMS tunable capacitor applications in mobile phones," in *Proceedings of the 10th IEEE International Conference on Solid-State and Integrated Circuit Technology (ICSICT '10)*, pp. 635–638, November 2010.

[32] M. G. S. Hossain and T. Yamagajo, "Reconfigurable printed antenna for a wideband tuning," in *Proceedings of the 4th European Conference on Antennas and Propagation (EuCAP '10)*, April 2010.

[33] S. Oh, H. Song, J. T. Aberle, B. Bakkaloglu, and C. Chakrabarti, "Automatic antenna-tuning unit for software-defined and cognitive radio," *Wireless Communications and Mobile Computing*, vol. 7, no. 9, pp. 1103–1115, 2007.

[34] A. Suyama and H. Arai, "Meander line antenna built in folder-type mobile," in *Proceedings of the International Symposium on Antennas and Propagation (ISAP '07)*, pp. 294–297, 2007.

[35] Y. Tsutsumi, M. Nishio, S. Obayashi et al., "Low profile double resonance frequency tunable antenna using RF MEMS variable capacitor for digital terrestrial broadcasting reception," in *Proceedings of the 2009 IEEE Asian Solid-State Circuits Conference*, pp. 125–128, November 2009.

[36] Computer Simulation Technology (CST), *CST Microwave Studio*, 2012, http://www.cst.com.

[37] A. D. Yaghjian and S. R. Best, "Impedance, bandwidth, and Q of antennas," *IEEE Transactions on Antennas and Propagation*, vol. 53, no. 4, pp. 1298–1324, 2005.

[38] S. R. Best, "Electrically small multiband antennas," in *Multiband Integrated Antennas for 4G Terminals*, D. A. Sanchez-Hernandez, Ed., chapter 1, pp. 1–32, Artech House, Norwood, Mass, USA, 2008.